PROCEEDINGS of the
23rd International Congress on Acoustics

9 to 13 September 2019 in Aachen, Germany

Defect detection using the identification of resonance frequency by spatial spectral entropy for noncontact acoustic inspection method

Kazuko SUGIMOTO[1]; Tsuneyoshi SUGIMOTO[2]; Noriyuki UTAGAWA[3]; Chitose KURODA[4]

[1,2] Toin University of Yokohama, Japan

[3,4] SatoKogyo Co., Ltd., Japan

ABSTRACT

In a noncontact non-destructive manner, our noncontact acoustic inspection method can detect and visualized internal defects (crack, peeling, cavity, etc.) in shallow layer of concrete from a long distance. The measurement surface was acoustically excited by airborne sound waves, and a two-dimensional vibration velocity distribution is measured by a highly sensitive scanning laser Doppler vibrometer (SLDV). When there is an internal defect, a flexural resonance occurs in a defective part, and vibration energy difference from a healthy part can be detected and imaged as vibrational energy ratio. If the resonance frequency range of an internal defects is known, a clear acoustic image can be generated by narrowing the analysis frequency range rather than using over the entire measurement frequency range. The resonance frequency in a measurement plane can be detected by 'spatial spectral entropy (SSE)' we proposed. In addition, in order to perform sound waves excitation, resonance may occur in a laser head of highly sensitive laser Doppler vibrometer due to the influence of reverberation from the surroundings. This resonance frequency can also be detected. It is necessary to perform acoustic imaging except for the resonance frequencies of the laser head.

Keywords: Noncontact acoustic inspection, NDT, Spatial spectral entropy, Laser Doppler vibrometer, LRAD

1. INTRODUCTION

In a closed space such as a large underground cavity, when detecting internal defects of concrete by noncontact acoustic inspection method, it is necessary to increase the sound pressure as the distance increases. Then, it is known that the reverberation from the surroundings cause resonance on the laser head of a high sensitivity scanning laser Doppler vibrometer (SLDV). In a closed space, resonance peaks of a laser head tend to be larger than that in a released space, and the frequency band of resonance also tends to widen. Because they adversely affect acoustic image visualized by vibrational energy, defect image is need to be calculated excluding the resonance frequency. The resonance frequency of internal defects of concrete is estimated to some extent from experience, and the frequency band of the transmitted sound waves is determined. But the real resonance frequency is not known in advance. For the measurement results, some resonance peaks can be seen by visual checking the vibration velocity spectrum at each measurement point one by one. However, there is no information on the frequency where the resonance frequency of the internal defect is found. And when the difference between the resonance peak and the noise floor is small, it is difficult to identify the resonance peak. It is also necessary to distinguish between the resonance peak of the internal defect and that of the laser head. By the SSE analysis using spatial spectral entropy we proposed, all the resonance frequency in the measurement plane can be detected and displayed in a Figure. Not only the resonance frequency of internal defects, but also that of the laser head of SLDV can be detected and identified.

[1] kazukosu@toin.ac.jp
[2] tsugimot@toin.ac.jp
[3] utagawa@satokogyo.co.jp
[4] kuroda@satokogyo.co.jp

2. EXPERIMENTAL METHOD

2.1 Experimental setup

Figure 1 shows the experimental setup. In order to detect Internal defects, such as a crack or a peeling, in shallow layer of concrete in noncontact non-destructive manner, strong plane waves were irradiated from a long-range acoustic device (LRAD; LRAD corp., LRAD-300X) installed at a distance of about 5 m from the measurement plane, and the concrete measurement surface was acoustically excited. A scanning laser Doppler vibrometer (SLDV; Polytec, RSV-500Xtra scanning vibrometer) was installed at a distance of 5-7 m from the measurement surface, and the two-dimensional vibration velocity distribution on the measurement plane was measured.

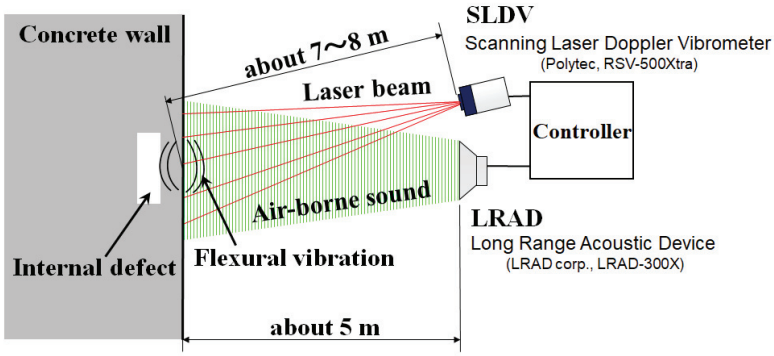

Figure 1 – Experimental setup

2.2 Signal processing

Using the difference in arrival time of the sounds and the light, the signal processing of 'Time-Frequency gate' was performed to reduce the noise caused by such as the direct waves from a sound source to a laser head and the reflected waves from the concrete measurement surface or the reverberation from the surroundings. As a transmission waveform, tone burst wave was used. It has sounding time and not sounding time. Sound changes in frequency step by step.

3. PRINCIPLE

3.1 Defect detection algorithm

When drawing a scatter diagram such as Figure 2 using two acoustical feature quantities (vibrational energy ratio and spectral entropy), measurement points in a healthy part of concrete show tendency to gather in an area where vibrational energy is low and spectral entropy is high. And the measurement points of defective part exist in the area with high vibrational energy and low spectral entropy. This defect detection algorithm was described in the reference (2).

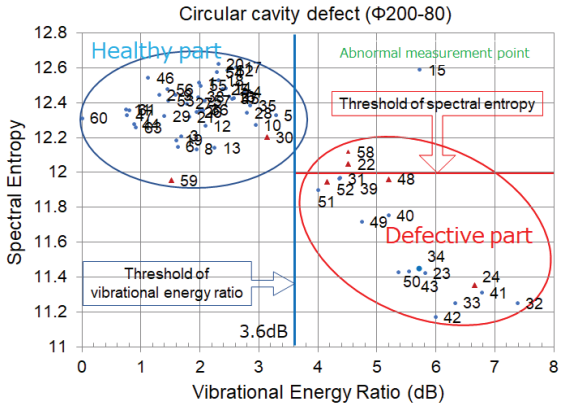

Figure 2 – Scatter diagram of vibrational energy ratio and spectral entropy

3.1.1 Vibrational energy ratio

The vibrational energy ratio is represented by the following equation (1) in the reference (1),

$$[VER]_{dB} = 10\log_{10}\frac{\int_{f_1}^{f_2}(PSD_{defect})df}{\int_{f_1}^{f_2}(PSD_{healthy})df} \quad (1)$$

where f_1 and f_2 are, respectively, the lower and upper limits of the analysis frequency within the frequency range of the transmitted airborne sound waves and *PSD* is the power spectral density. The ratio of vibrational energy of defective part to vibrational energy of a healthy part of concrete is calculated in the measurement frequency range.

3.1.2 Spectral entropy

The spectral entropy (SE) is represented as H by the following equation (2),

$$H = -\sum_f P_f \, log_2 \, P_f \qquad P_f = \frac{S_f}{\sum_f S_f} \quad (2)$$

where S_f is the power spectrum of the vibration velocity at a measured point. The spectral entropy expresses the white characteristic of the signal. The spectrum of the signal is regarded as a probability distribution and the information entropy is calculated.

3.1.3 Statistical evaluation of a healthy part of concrete

Each distribution of acoustic feature quantity (vibrational energy ratio and spectral entropy) in a healthy part of concrete tends to show a normal distribution as stated in the reference (3).

3.2 Spatial Spectral Entropy (SSE)

The spectral entropy (SE) is a feature quantity that expresses the whiteness of a signal, assuming the signal spectrum as a probability distribution and calculating information entropy. SE has a high value in a signal having a uniform spectrum such as a white noise, and a low value in a signal in which the spectrum like a voice signal is not uniform.

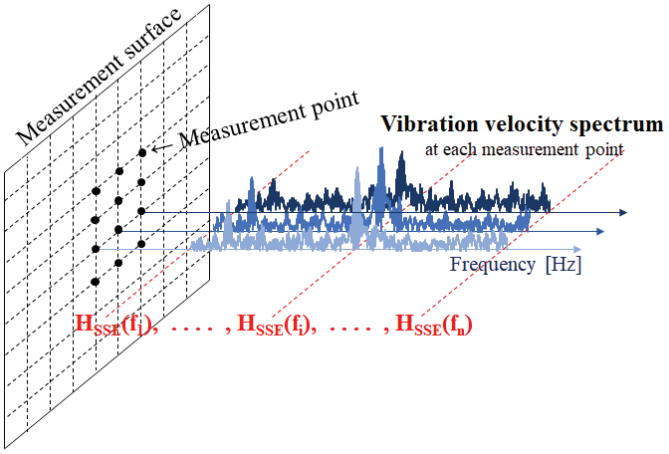

Figure 3 – Illustration of 'Spatial Spectral Entropy (SSE)'

As shown in Figure 3, consider the frequency axis of vibration velocity spectrum perpendicular to the measurement plane. Several examples of vibration velocity spectrum at a measured point are displayed from each measured point in the direction perpendicular to the measurement surface. We propose a method of simultaneously detecting not only the resonance frequency of internal defects but also the resonance frequency of a laser head of SLDV by calculating the $H_{SSE}(f)$ on a planar measurement plane. The SE expanded to such a planar measurement plane is referred to as 'Spatial Spectral Entropy (SSE)' and is defined by the following equation (3) in the reference (4).

$$H_{SSE}(f) = -\sum_{i=1}^{m}\sum_{j=1}^{n} P_{i,j}(f) \, log_2 \, P_{i,j}(f) \quad (3)$$

$$P_{i,j}(f) = \frac{S_{i,j}(f)}{\sum_{i=1}^{m}\sum_{j=1}^{n} S_{i,j}(f)}$$

Where $H_{SSE}(f)$ is spectral entropy (a function of frequency f) extended to real space. For example,

when considering a two-dimensional measurement plane, the grating measured point $r(x,y)$ is expressed as an array $r_{i,j}$ $(i = 1,m\,;\; j = 1,n)$. $S_{i,j}(f)$ is the spatial frequency component f [Hz] of the power spectrum obtained by performing discrete Fourier transform on the signal measured at the measurement point $r_{i,j}$. $P_{i,j}(f)$ is the probability that the spatial frequency component f [Hz] of the power spectrum at the measurement point $r_{i,j}$ exists within the measured plane. Therefore, $H_{SSE}(f)$ indicates the information entropy calculated for the frequency component f of vibration velocity spectrum at all measured points.

4. EXPERIMENTAL RESULTS

4.1 Specimen with circular peeling defects

Internal defects of concrete include a different shape of defect such as a crack, a peeling, or a cavity. We investigated peeling defects that were more difficult to detect than the same size of cavity defect. Figure 4 shows the shape, size, and burial depth of peeling defects.

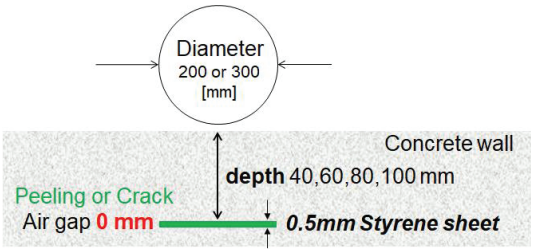

Figure 4 – Position and size of a circular peeling defect embedded in concrete

4.2 Analysis results of spatial spectral entropy and acoustic visualization of defects

4.2.1 Circular peeling defect (diameter = 200 mm, burial depth = 40mm)

Figure 5 shows the result of SSE analysis from the vibration velocity data obtained by noncontact acoustic inspection method for a circular peeling defect (diameter 200 mm, burial depth 40 mm).

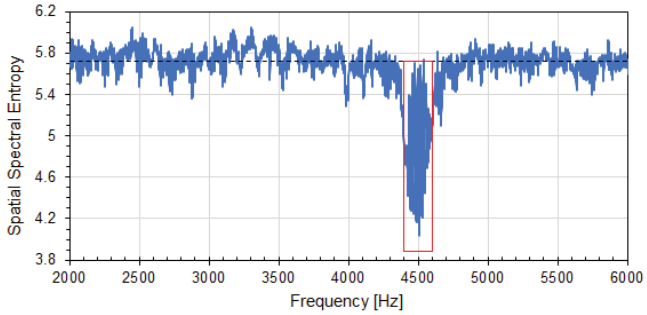

Figure 5 – Analysis result by spatial spectral entropy (SSE)

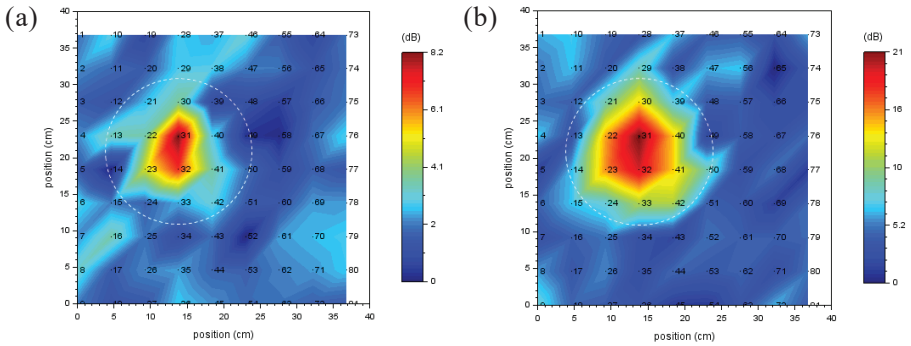

Figure 6 – Acoustic visualization of circular peeling defect (Φ200, 40) by vibrational energy ratio
Frequency band for imaging (a) 2000-6000Hz, (b) 4400-4600Hz

A resonance peak is observed around the frequency 4500 Hz in the figure. The black dotted line in the

figure is the median of SSE value, 5.72, in the measurement frequency range (2000-6000 Hz).

Figure 6 is an acoustic image of a circular peeling defect. The frequency range for imaging of (a) was 2000-6000 Hz, and that of (b) was 4400-4600 Hz. Based on the SSE result, vibrational energy ratio was calculated in a narrower frequency range and (b) was visualized. The white dotted circle in Figure 6 shows the size and approximate position of the defect. The area of a peeling defect is more faithfully reproduced in (b) than in (a). Max color scale in (b) is 21 dB, which is larger than 8.2 dB in (a). The difference of vibrational energy ratio between the defective part and the healthy part of concrete looks larger in (b) than in (a). Therefore, defect image of (b) looks more clearly than that of (a).

4.2.2 Circular peeling defect (diameter = 200 mm, burial depth = 60mm)

Figure 7 shows the result of SSE analysis from the vibration velocity data obtained by noncontact acoustic inspection for a circular peeling defect (diameter 200 mm, burial depth 60 mm). A resonance peak is observed in the frequency range 4000-4500 Hz in red frame of the figure. The black dotted line in the figure is the median of SSE value, 5.65, calculated in the measurement frequency range (2000-6000 Hz).

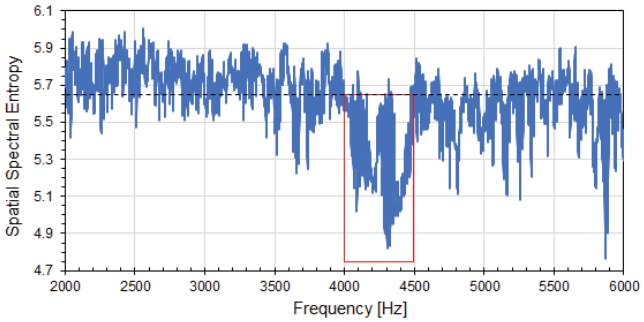

Figure 7 – Analysis result by spatial spectral entropy (SSE)

Figure 8 is an acoustic image of a circular peeling defect. The frequency range for imaging of (a) was 2000-6000 Hz, and that of (b) was 4000-4500 Hz. Based on the SSE result, vibrational energy ratio was calculated in a narrower frequency range and (b) was visualized. The dotted circle in Figure 8 shows the size and approximate position of the defect. The area of a peeling defect is more faithfully reproduced in (b) than in (a). Color scale in (b) is 17 dB, which is larger than 8 dB in (a). The difference of vibrational energy ratio between the defective part and the healthy part looks larger in (b) than in (a). Therefore, defect image of (b) looks more clearly than that of (a).

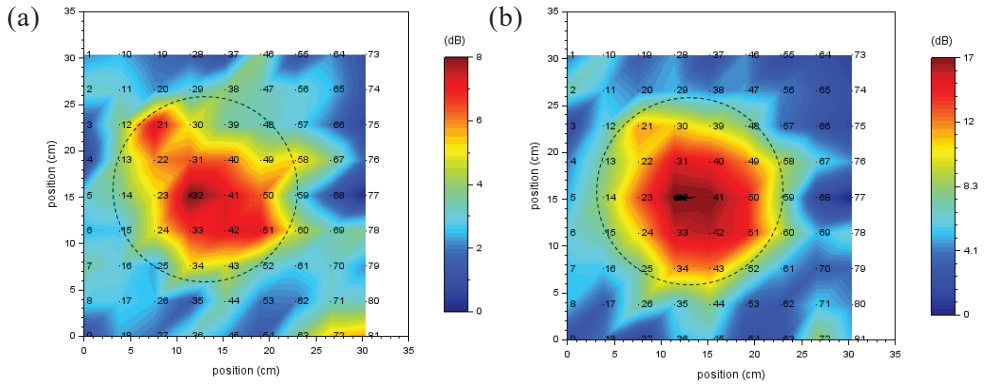

Figure 8 – Acoustic visualization of circular peeling defect (Φ200, 60) by vibrational energy ratio
Frequency band for imaging (a) 2000-6000Hz, (b) 4000-4500Hz

4.2.3 Circular peeling defect (diameter = 300 mm, burial depth = 40 mm)

Figure 9 shows the result of SSE analysis from the vibration velocity data obtained by noncontact acoustic inspection method for a circular peeling defect (diameter 300 mm, burial depth 40 mm). A resonance peak is observed in the frequency range 1800-2400 Hz in red frame of the figure. The black dotted line in the figure is the median of SSE value, 5.64, calculated in the measurement frequency range (2000-6000 Hz).

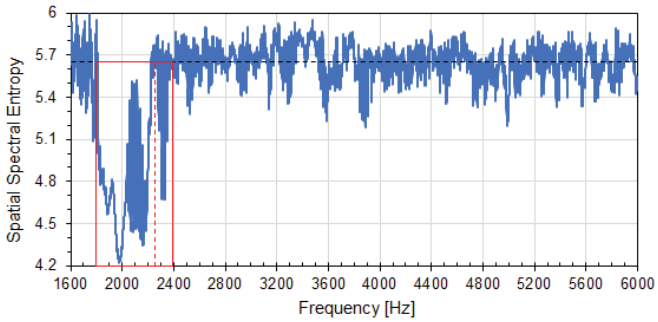

Figure 9 – Analysis result by spatial spectral entropy (SSE)

Figure 10 is acoustic images of a circular peeling defect. (a) was visualized in the measurement frequency range of 2000-6000 Hz. Based on the SSE result, it can be seen that the resonance frequency range started from the frequency 1800Hz lower than the measurement frequency 2000Hz. Moreover, vibrational energy ratio was calculated in a narrower frequency range and the acoustic images of the defect were visualized. Therefore, in (b) the frequency range for imaging was 1800-2250 Hz, and in (c) the frequency range was 1800-2400 Hz. The upper right part of the peeling defect in (a) is missing, but in (b) and (c), the missing part looks to be compensated by setting the start frequency to 1800 Hz. Although (b) looks the same as (c), max color scales were 26 dB in (b), 23 dB in (c), which were larger than 11 dB in (a). The difference of vibrational energy ratio between the defective part and the healthy part of concrete looks largest in (b) compared the others. Therefore, a clearer image is obtained in (b). The dotted circle in Figure 10 shows the size and approximate position of the defect. The area of a peeling defect is more faithfully reproduced in (b), (c) than in (a).

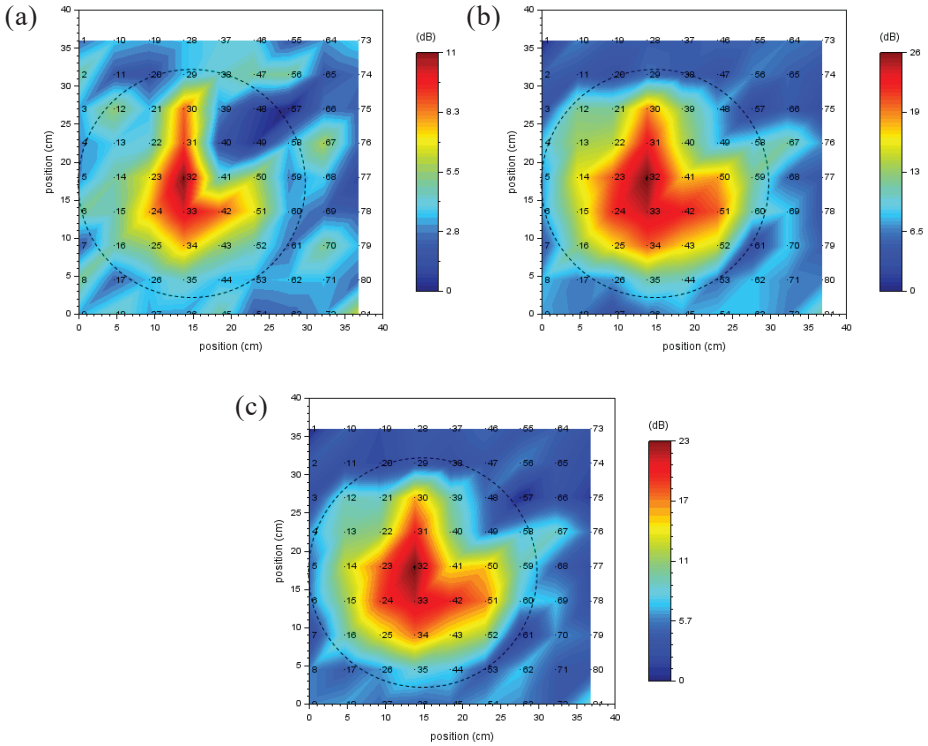

Figure 10 – Acoustic visualization of circular peeling defect (Φ300, 40) by vibrational energy ratio
Frequency band for imaging (a) 2000-6000Hz, (b) 1800-2250Hz, (c) 1800-2400Hz

4.2.4 Circular peeling defect (diameter = 300 mm, burial depth = 60 mm)

Figure 11 shows the result of SSE analysis from the vibration velocity data obtained by noncontact acoustic inspection method for a circular peeling defect (diameter 300 mm, burial depth 60 mm). A resonance peak is observed in the frequency range 2550-2850 Hz in red frame of the figure. The black dotted line in the figure is the median of SSE value, 5.71, calculated in the measurement frequency range (1000-4800 Hz).

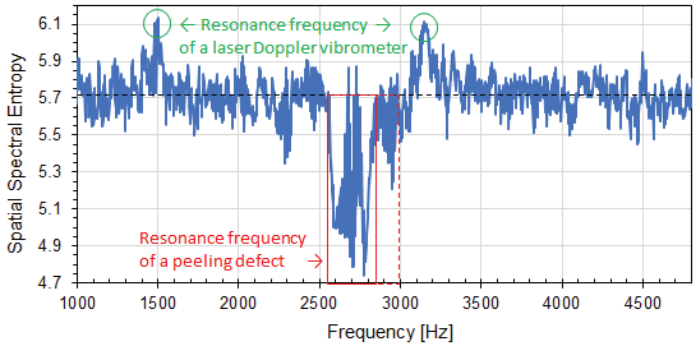

Figure 11 – Analysis result by spatial spectral entropy (SSE)

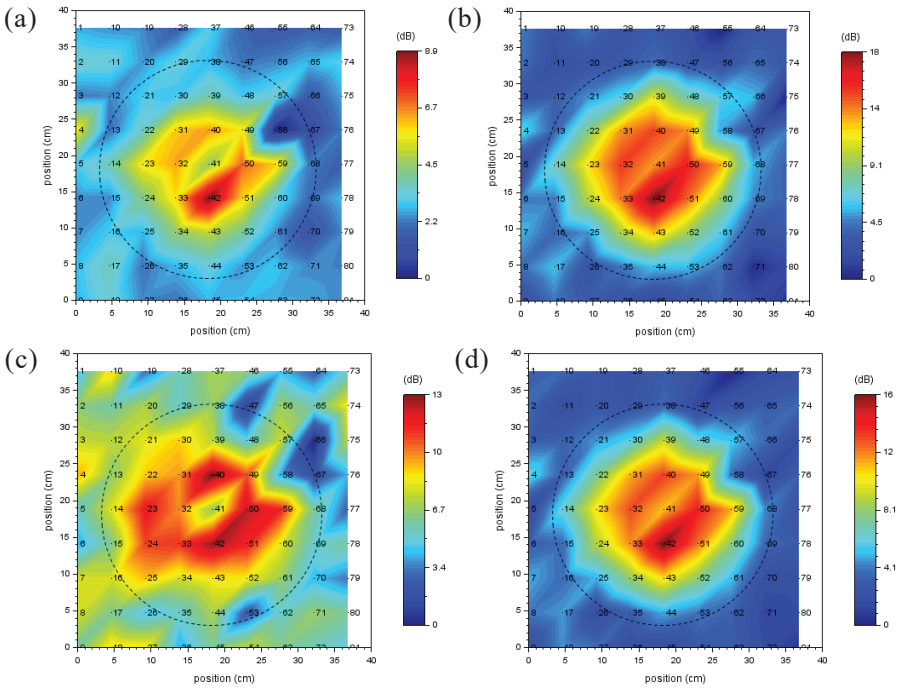

Figure 12 – Acoustic visualization of circular peeling defect (Φ300, 60) by vibrational energy ratio
Frequency band for imaging (a)1000-4800Hz, (b)2550-2850Hz, (c)2850-3000Hz, (d)2550-3000Hz

4.3 Summary and discussion

From the above, the relationship between resonance frequency of circular peeling defect and the diameter or buried depth of the defect is, in the condition of this experiment, as shown in Table 1.

Table 1 Relationship between resonance frequency range of circular peelings and diameter or buried depth

Diameter of circular peeling [mm]		200			300		
Resonance frequency [Hz]		Lower limit	Representative value (Local minimum of SSE)	Upper limit	Lower limit	Representative value (Local minimum of SSE)	Upper limit
Burial depth [mm]	40	4400	4507.7	4600	1800	1975.9	2200
	60	4020	4304.9	4500	2550	2774.2	2850
	80	4220	4349.4	4450	2950	3046.0	3150
	100				3250	3382.7	3450

A circular peeling defect was considered to have a certain range of resonance frequency, not a single resonance frequency. That frequency range was thought to be broader than that of a circular cavity defect. In Table 1, the local minimum of SSE is shown as a representative value. The range of resonance frequency is indicated by the lower limit value and the upper limit value.
The above results are summarized as shown in Figure 13. From this figure, in case of a circular peeling defect with a diameter of 300 mm, as the burial depth increases from 40 to 100 mm, the resonance frequency increases in proportion. That is, as the depth of a circular peeling defect is deeper, the

resonance frequency becomes higher, however in the range of conditions such as these diameter and depth. In addition, the resonance frequency is higher at a circular peeling defect with a diameter of 200 mm than that of 300 mm. That is, the smaller the cross-sectional area of the peeling defect, the higher the resonance frequency. The dotted line in the figure is a result of linear least squares fitting.

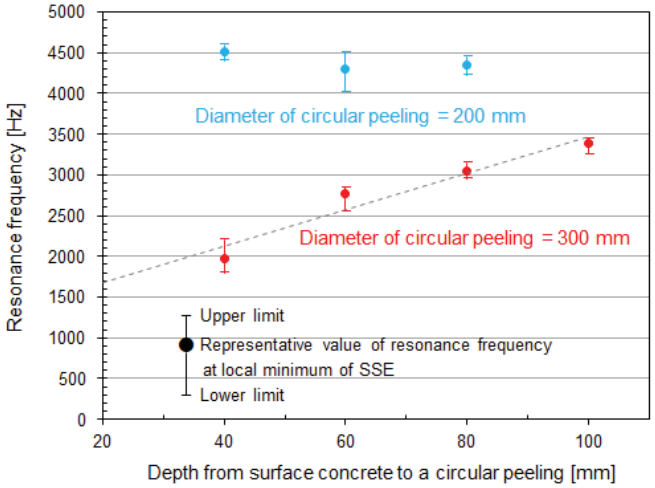

Figure 13 – Relation between resonance frequency of circular peeling defect and diameter or burial depth

In our noncontact acoustic inspection method, flexural resonance is assumed as a vibration state of cavity or peeling defect. As the theoretical formula of flexural resonance of a solid circular plate (clamped all around or simply supported all around), the natural frequency is known as

$$f_{mn} = \frac{1}{2\pi}\frac{\lambda_{mn}}{a^2}\sqrt{\frac{Eh^2}{12(1-\nu^2)\rho}} \tag{4}$$

where f_{mn}: natural frequency [Hz], E: Young's modulus [Pa], a: radius of disk [m], ρ: mass per unit volume [kg/m^3], h: plate thickness [m], ν: Poisson's ratio, m: number of nodal circles, n: number of nodal diameters.

In a peeling defect in the shallow layer of concrete, although there exists no void around peeling, since it is applied to the theoretical formula of flexural resonance of a flat disk under this experimental condition, it can be seen that flexural vibration actually occurs. If the concrete measurement surface can be acoustically excited enough, the phenomenon of flexural resonance may be able to be caught.

5. CONCLUSIONS

In noncontact acoustic inspection method, using remotely measured vibration velocity data, spatial spectral entropy (SSE) analysis can detect the resonance frequencies and those frequency range in the measurement plane. By identify the resonance frequency and narrowing the frequency range for imaging, acoustic image of a circular peeling defect in shallow layer of concrete was visualized clearly.

ACKNOWLEDGEMENTS

This work was supported by JSPS KAKENHI Grant Numbers 17K06542.

REFERENCES

1. Katakura K, Akamatsu R, Sugimoto T, Utagawa N. Study on detectable size and depth of defects in noncontact acoustic inspection method. Jpn. J. Appl. Phys. 2014, 53, 07KC15.
2. Sugimoto K, Akamatsu R, Sugimoto T, Utagawa N, Kuroda C, Katakura K. Defect-detection algorithm for noncontact acoustic inspection using spectrum entropy. Jpn. J. Appl. Phys. 2015, 54, 07HC15
3. Sugimoto K, Sugimoto T, Utagawa N, Kuroda C, and Kawakami A. Detection of internal defects of concrete structures based on statistical evaluation of healthy part of concrete by the noncontact acoustic inspection method. Jpn. J. Appl. Phys. 2018, 57, 07LC13.
4. Sugimoto K, Sugimoto T, Utagawa N, Kuroda C. Detection of resonance frequency of both the internal defects of concrete and the laser head of a laser Doppler vibrometer by spatial spectral entropy for noncontact acoustic inspection. to be published in Jpn. J. Appl. Phys. 2019; 58.